The results are

$$L_1^2=[3-3L_1^0]/w,$$
$$L_1^4=[(5/3)w-5+5L_1^0]/w^2,$$
$$L_1^6=[(7/5)w^2-(7/3)w+7-7L_1^0]/w^3,$$
$$L_2^0=[(1/2)L_1^0+(1/2)/(1+w)],$$
$$L_2^2=[(3/2)L_1^0-(3/2)/(1+w)]/w,$$
$$L_2^4=[5-(15/2)L_1^0+(5/2)/(1+w)]/w^2,$$
$$L_2^6=[(7/3)w-14+(35/2)L_1^0-(7/2)/(1+w)]/w^3,$$
$$L_3^2=[(3/8)L_1^0+(3/8)/(1+w)-(3/4)/(1+w)^2]/w,$$
$$L_3^4=[(15/8)L_1^0-(25/8)/(1+w)+(5/4)/(1+w)^2]/w^2,$$
$$L_3^6=[7-(105/8)L_1^0+(63/8)/(1+w)-(7/4)/(1+w)^2]/w^3, \quad \text{(B9)}$$

and

$$L_3^8=[3w-27+(315/8)L_1^0-(117/8)/(1+w)+(9/4)/(1+w)^2]/w^4.$$

PHYSICAL REVIEW VOLUME 152, NUMBER 2 9 DECEMBER 1966

R Center in KCl: Electron-Spin-Resonance Studies of the Ground State*

D. C. KRUPKA† AND R. H. SILSBEE‡
Laboratory of Atomic and Solid State Physics and Department of Physics, Cornell University, Ithaca, New York

(Received 23 June 1966)

A calculation of the g tensor is carried out for the ^2E ground state of the R center in KCl. The method employs linear combinations of atomic orbitals as wave functions, made up of F-center $1s$ states orthogonalized to the occupied states of the crystal, and takes into account the dynamical Jahn-Teller effect and the "many-center" nature of the problem. The positive sign of the g shift $\delta g_{\|}$ is correctly predicted, and the magnitude is in reasonable agreement with experiment. From studies of the stress dependence of $\delta g_{\|}$, a value is obtained for the strength of the Jahn-Teller coupling, which is found to be $k^2=3.0\pm0.5$ in the notation of Longuet-Higgins, Öpik, Pryce, and Sack. The effects of random internal strains are found to play an important role, broadening the signal beyond observability at zero applied stress. Estimates of the R-center spin-lattice relaxation rate fall considerably short of the experimental value, for which an upper limit is obtained from saturation plots. Experiments to determine the effect of the presence of the R center on the spin-lattice relaxation rate of the F center indicate that the R center forms a significant channel for F-center relaxation at large R concentrations, and may not be dismissed as a possible relaxation channel at very low R concentrations.

I. INTRODUCTION

IN an earlier publication,[1] the observation of an electron-spin-resonance (ESR) signal identified with the R center in KCl was reported. The results of the initial experiments gave considerable support to the van Doorn model[2] of the R center: three F centers in an equilateral triangular arrangement with a ⟨111⟩ symmetry axis (see Fig. 1). Subsequent work by Silsbee[3] (hereinafter referred to as I), and Seidel, Schwoerer, and Schmid[4] has further demonstrated the validity of the model. The purpose of this paper is to describe additional ESR experiments on this system, and to set up a theory to explain the main features of the resonance. This work complements the optical studies of I and draws on the theoretical framework set up in that paper

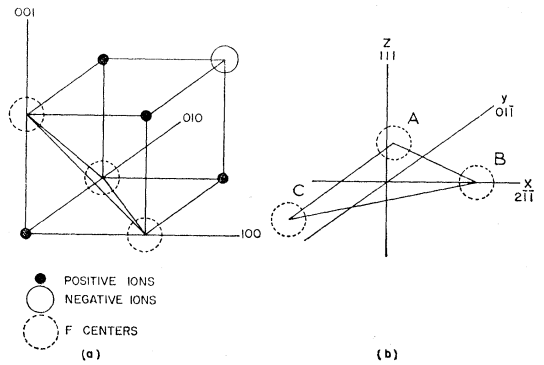

FIG. 1. The van Doorn model of the R center. (a) Ionic configuration. (b) Local axes for a [111] R center.

* Work supported by the U. S. Atomic Energy Commission.
† Present address: Clarendon Laboratory, University of Oxford, Oxford, England.
‡ On leave 1965–66, Swiss Federal Institute, Zürich, Switzerland.
[1] D. C. Krupka and R. H. Silsbee, Phys. Rev. Letters **12**, 193 (1964).
[2] C. Z. van Doorn, Philips Res. Rept. Suppl. 4, (1962).
[3] R. H. Silsbee, Phys. Rev. **138**, A180 (1965).
[4] H. Seidel, M. Schwoerer, and D. Schmid, Z. Physik **182**, 398 (1965).

Summarized below are the salient features of the resonance signal as they were first reported[1]:

1. The signal is observed only at low temperatures (in the liquid-helium range) and under large applied uniaxial stress, σ_{app} ($\sigma_{app} \approx 2$ kg/mm^2).
2. The angular variation of the g value is consistent with a center having a ⟨111⟩ symmetry axis.
3. The g shift $\delta g_{\parallel}$ is *positive*, while $\delta g_{\perp} \approx 0$.

After a brief symmary of the experimental details in Sec. II, the g tensor is considered in Sec. III. A calculation of the g is carried out using the wave functions introduced in I and the results are used to interpret the features summarized above, as well as further data on the stress dependence of the g tensor. Section IV presents simple considerations of spin-relaxation processes and data obtained on the relaxation times T_1 and T_2 by saturation experiments. The influence of R centers as possible relaxation channels for F centers is treated in Sec. V.

II. EXPERIMENTAL DETAILS

Harshaw KCl was used in all experiments. The crystals were ground using simple jigs to dimensions roughly 15×3.5×3.5 mm. The long axis being in the [110] direction, the faces (1$\bar{1}$0) and (001). Annealing was carried out by holding the crystals at 600°C for 1 h under chlorine introduced at 100°C at 1 atm, and then slowly (2°C/min) cooling to room temperature. All crystals were colored by x irradiation at 150 kV peak and 12 mA, with soft x rays filtered out by 0.3 mm of aluminum. Bleaching was usually accomplished by placing the sample under a fluorescent lamp and was continued until the R bands peaked. A Cary Model 14R Spectrophotometer was used to monitor the optical absorption with all measurements carried out at room temperature. A typical F-center density was about 10^{17} cm^{-3}.

In some experiments, preferentially oriented R centers were required.[5] In such instances, crystals were ground with ($\bar{1}$11) and (1$\bar{1}$2) faces. Bleaching light in the R_2 band polarized in the [$\bar{1}$11] direction with k vector in the [1$\bar{1}$2] direction was then used to populate the [$\bar{1}$11] R centers at the expense of the three other equivalent orientations.

The spectrometer, of standard design, operated at 9 Gc/sec using balanced bolometer detection. For applying stress to the sample while studying ESR a TE_{101} cavity similar to Känzig's[6] was used, the stress being applied using a simple arrangement with lever and weights. The friction in the system was estimated to be equal to a force on the crystal of approximately 2 kg.

[5] F. Okamoto, Phys. Rev. **124**, 1090 (1961).
[6] W. Känzig, J. Phys. Chem. Solids **23**, 479 (1962).

III. THE g TENSOR

A. Vibronic States of the R Center

In calculating the g tensor, use will be made of the vibronic states of the R center given in I. These states are essentially those of Longuet-Higgins, Öpik, Pryce, and Sack[7] (LHOPS) and this paper draws heavily upon their results. For the sake of convenience, the eigenfunctions will be briefly summarized. For details the reader is referred to I and LHOPS.

The electronic ground state of the R center is of ^2E symmetry, the orbital degeneracy implying the possibility of a Jahn-Teller effect.[8] Distortions of E symmetry, which may be written as $Q_{2a}=r\cos\phi$ and $Q_{2b}=r\sin\phi$ in normal coordinate space, will lift the electronic degeneracy giving the double-sheeted Born-Oppenheimer potential of Fig. 2. The strength of the coupling is given by the parameter k^2 such that the potential minimum is lowered by an amount $\frac{1}{2}k^2$ in units of $\hbar\omega_E$ where ω_E is the frequency of the E modes.

The vibronic functions derived from the ground electronic state may be written[3]

$$\Psi_{xpl}=(2\pi)^{-1/2}\mathcal{E}_x[u_{pl}(-r)\cos l\phi\cos(\tfrac{1}{2}\phi)+(-)^{l-1/2}u_{pl}(r)\times\sin l\phi\sin(\tfrac{1}{2}\phi)]+(2\pi)^{-1/2}\mathcal{E}_y[u_{pl}(-r)\cos l\phi\times\sin(\tfrac{1}{2}\phi)-(-)^{l-1/2}u_{pl}(r)\sin l\phi\cos(\tfrac{1}{2}\phi)], \quad (1)$$

$$\Psi_{ypl}=(2\pi)^{-1/2}\mathcal{E}_x[u_{pl}(-r)\sin l\phi\cos(\tfrac{1}{2}\phi)-(-)^{l-1/2}\times u_{pl}(r)\cos l\phi\sin(\tfrac{1}{2}\phi)]+(2\pi)^{-1/2}\mathcal{E}_y[u_{pl}(-r)\times\sin l\phi\sin(\tfrac{1}{2}\phi)+(-)^{l-1/2}u_{pl}(r)\cos l\phi\cos(\tfrac{1}{2}\phi)].$$

$\mathcal{E}_x$ and $\mathcal{E}_y$ are the pair of degenerate electronic wave functions, even and odd, respectively, under reflection in the xz plane of Fig. 1; $u_{pl}(-r)$ and $u_{pl}(r)$ are radial wave functions discussed by LHOPS.

The quantum numbers required to specify completely the vibronic state are the electronic state, the over-all symmetry in the xz plane (x or y), the radial quantum number p which has a physical interpretation for large k^2 in terms of radial excitations across the trough of

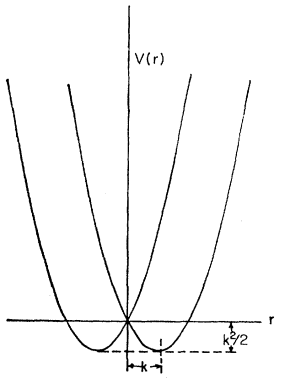

FIG. 2. The Born-Oppenheimer surfaces for a twofold degenerate electronic level.

[7] H. C. Longuet-Higgins, U. Öpik, M. H. L. Pryce, and R. A. Sack, Proc. Roy. Soc. (London) **244**, 1 (1958).
[8] H. A. Jahn and E. Teller, Proc. Roy. Soc. (London) **A161**, 220 (1937).

Fig. 2, and the half-integer quantum number l which describes rotation around the trough. The quantum numbers p take on the values 1, 2, 3, $\cdots$, while l the values $\frac{1}{2}, \frac{3}{2}, \frac{5}{2}, \cdots$. The degenerate pair of ground-state vibronic wave functions, Ψ_{xpl} and Ψ_{ypl}, transform as E for $l=\frac{1}{2}$.

For the ground-state electronic wave functions $\mathcal{E}_x$ and $\mathcal{E}_y$, Heitler-London wave functions will be used as a first approximation.

$$|\mathcal{E}_x+\rangle=(1/\sqrt{2})[a_+(1)c_-(2)b_+(3)-b_+(1)a_-(2)c_+(3)],$$
$$|\mathcal{E}_y+\rangle=(1/\sqrt{6})[2c_+(1)b_-(2)a_+(3)+b_+(1)c_-(2)a_+(3)+c_+(1)a_-(2)b_+(3)], \quad (2)$$

where $a_+(1)c_-(2)b_+(3)$ stands for a 3×3 Slater determinant, and where $a_+(i)$ is a one-electron spin orbital for the F center at A (see Fig. 1) with spin quantum number $m_s=+\frac{1}{2}$. In particular, the F-center wave functions will take the form[9]

$$a=(a_s-\sum_{k,\alpha}\langle a_s|\phi_{k\alpha}\rangle\phi_{k\alpha})(1-\sum_{k,\alpha}\langle a_s|\phi_{k\alpha}\rangle^2)^{-1/2}, \quad (3)$$

where a_s refers to the normalized s-like F-center wave function before it is made orthogonal to the occupied orbitals of the neighboring ions; $\phi_{k\alpha}$ refers to orbital α on ion k. For the sake of compactness $\langle a_s|\phi_{k\alpha}\rangle$ will be written $\Omega_{ak\alpha}$.

It is to be noted that the orbitals in the Slater determinants are nonorthogonal. This fact will be reflected when considering matrix elements of one-electron operators. Strictly speaking, the nonorthogonality also enters the normalization but the effect is small and will be neglected.

B. Calculation of the g Tensor

The behavior of the lowest lying quartet of states of ^2E symmetry, with a twofold orbital or vibronic and twofold spin degeneracy, when subjected to magnetic and strain fields can be described in terms of an effective Hamiltonian. This Hamiltonian is developed from the electronic Hamiltonian

$$\mathcal{H}=\mathcal{H}_{ST}+\mathcal{H}_{OZ}+\mathcal{H}_{SZ}+\mathcal{H}_{SO}, \quad (4)$$

where the terms refer, respectively, to the electronic interaction with the strain field, the orbital Zeeman interaction, the spin-Zeeman interaction, and the spin-orbit interaction. The phenomenology of the strain term in the effective Hamiltonian is developed in I and a simplified form is used here since the experiments were all performed with the stress along a single direction, the crystal [110] axis. The strength of the strain coupling is not calculated but taken from the empirical results of I. The contributions of the three magnetic interaction terms to an effective Hamiltonian are developed using the wave functions described above. The calculation is carried out under the simplifying assumption that the neighboring ions are not displaced from their positions in a perfect crystal ("unrelaxed" model).

Two types of terms contribute to the constants of the effective Hamiltonian. The first involve the matrix elements of the Hamiltonian (4) within the ^2E ground state. In calculating these elements it is assumed that both the operators and the electronic states are independent of the vibrational coordinates, i.e., the wave functions are assumed of the form described by LHOPS and introduced in the preceding section. The elements of (4) among the vibronic states then occur as the product of the pure electronic matrix element and a vibrational overlap integral. The magnitude of the vibrational overlap depends sensitively upon the vibrational coupling, and, for a moderate to strong Jahn-Teller effect, there is a marked reduction in the orbital moment and spin-orbit energy. Along with the reduction of matrix elements within the ground ^2E state, there is a corresponding increase in the matrix elements of (4) between the ground state and excited vibronic states with $p>1$ and $l=\frac{1}{2}$. This leads to admixtures of these higher states into the ground state by the spin-orbit interaction and contributes to a g shift which may be calculated by second-order perturbation theory. Ham[10] has recently discussed both the reduction of the spin-Hamiltonian parameters and the closely related enhanced second-order effects.

With a many-center imperfection such as the R center, care must be taken to insure that the g tensor be gauge-invariant. This problem has been considered by Stone[11] and the results of his calculation may be summarized for present purposes as follows:

The angular-momentum operator is taken as $\sum_i \mathbf{l}_{0i}$ where $\mathbf{l}_{0i}$ is the angular-momentum operator for electron i taken about the origin which is taken to be, in this case, the centroid of the equilateral configuration of F centers. Thus, the vector potential $\mathbf{A}$ is written $\mathbf{A}=\frac{1}{2}\mathbf{H}\times\mathbf{r}$, where $\mathbf{r}$ is the position vector of an electron relative to the centroid of the system. The spin-orbit operator is written $\sum_{k,i}\xi_k\mathbf{l}_{ki}\cdot\mathbf{s}_i$, where $\mathbf{l}_{ki}$ is the angular-momentum operator for electron i taken about ion k, and where ξ_k is the effective spin-orbit coupling constant for the ion k and will be defined more precisely in the following section. The calculated effective Hamiltonian takes the form

$$\mathcal{H}_{\text{eff}}=-\Delta(\sigma)(\Lambda_x^2-\Lambda_y^2)+\beta g_{OR}\Lambda_z H_z+\beta\mathbf{S}\cdot\mathbf{g}\cdot\mathbf{H}-\lambda_R\Lambda_z S_z, \quad (5)$$

appropriate for a system in which there is complete quenching of the x and y components of angular momentum by a strong axial field but in which the axial symmetry is removed only by the term involving the applied stress, σ. The pertinent matrices of the

[9] D. Y. Smith, Phys. Rev. **137**, A574 (1965).

[10] F. S. Ham, Phys. Rev. **138**, A1727 (1965).

[11] A. J. Stone, Proc. Roy. Soc. (London) **A271**, 424 (1963).

orbital operator Λ, diagonal in the effective spin, are

$$\Lambda_Z=\begin{Bmatrix}0 & -i\\ i & 0\end{Bmatrix};\quad \{\Lambda_x^2-\Lambda_y^2\}=\begin{Bmatrix}\frac{1}{2} & 0\\ 0 & -\frac{1}{2}\end{Bmatrix} \tag{6}$$

in the representation with the basis states the $\Psi_{x1\frac{1}{2}}$ and $\Psi_{y1\frac{1}{2}}$ defined earlier.

The strain splitting $\Delta(\sigma)$ is obtained knowing the applied [110] stress and the empirical coupling constant from I of 2.2 cm^{-1} for a stress of 1 kg/mm^2. The reduced orbital g value, g_{OR}, and the reduced spin-orbit parameter λ_R are calculated as follows:

$$\begin{aligned}\lambda_R&=2i\langle\Psi_{y1\frac{1}{2}}+|\mathcal{H}_{SO}|\Psi_{x1\frac{1}{2}}+\rangle\\&=2i\langle\Psi_{y1\frac{1}{2}}+|\sum_{k,i}\xi_k\mathbf{l}_{ki}\cdot\mathbf{s}_i|\Psi_{x1\frac{1}{2}}+\rangle;\end{aligned} \tag{7}$$

$$\begin{aligned}g_{OR}&=-i\langle\Psi_{y1\frac{1}{2}}+|\mathcal{H}_{OZ}|\Psi_{x1\frac{1}{2}}+\rangle\\&=-i\langle\Psi_{y1\frac{1}{2}}+|\sum_i l_{0i}{}^z|\Psi_{x1\frac{1}{2}}+\rangle.\end{aligned} \tag{8}$$

The evaluation of these elements, as noted above, is simplified by the factorization into the purely electronic elements evaluated in the following section,

$$\lambda_E=2i\langle\mathcal{E}_y+|\sum_{k,i}\xi_k\mathbf{l}_{ki}\cdot\mathbf{s}_i|\mathcal{E}_x+\rangle \tag{9}$$

$$g_{OE}=-i\langle\mathcal{E}_y+|\textstyle\sum_i l_{0i}{}^z|\mathcal{E}_x+\rangle, \tag{10}$$

and the Jahn-Teller reduction factor

$$f_{11}=\lambda_R/\lambda_E=g_{OR}/g_{OE}. \tag{11}$$

Here f_{11} is the vibrational overlap for $p=1$ obtained from

$$f_{1p}=\langle\rho_{1\frac{1}{2}}{}^+|\rho_{p\frac{1}{2}}{}^+\rangle-\langle\rho_{1\frac{1}{2}}{}^-|\rho_{p\frac{1}{2}}{}^-\rangle, \tag{12}$$

where the functions $\rho_{1\frac{1}{2}}{}^+$ and $\rho_{1\frac{1}{2}}{}^-$ are radial wave functions defined by LHOPS.

The remaining constant in the effective Hamiltonian is the $\mathfrak{g}$ tensor occurring in the spin-Zeeman term. This will be the free-electron g plus the second-order contributions obtained in Appendix IA. As shown there, these second-order terms contribute a positive

$$\delta\mathfrak{g}^{zz}=2\lambda_E g_{OE}\sum_{p=2}^{\infty}\frac{(f_{1p})^2}{E_{yp\frac{1}{2}}-E_{x1\frac{1}{2}}} \tag{13}$$

to the zz component of the $\mathfrak{g}$ tensor, and zero to the xx and yy components.

If, as in the case of the experiments, $\lambda_R\gg g_{OR}\beta H$, the lowest pair of energy levels of the effective Hamiltonian (5) show a Zeeman splitting described by a g tensor with principal values

$$g_{||}=2+2\lambda_E g_{OE}\left[\frac{f_{11}{}^2}{(\Delta^2+\lambda_R{}^2)^{1/2}}+\sum_{p=2}^{\infty}\frac{(f_{1p})^2}{E_{yp\frac{1}{2}}-E_{x1\frac{1}{2}}}\right] \tag{14}$$

and

$$g_\perp=2[1+\lambda_R{}^2/\Delta^2]^{-1/2}. \tag{15}$$

It is this g tensor which should be observed in an ESR experiment.

C. Evaluation of Basic Matrix Elements

(a) *Calculation of* λ_E

Using the Heitler-London wave functions of (2), it is readily shown that

$$\lambda_E=-\sqrt{3}i(Q^2+2Q)\langle a|\sum_k\xi_k l_k{}^z|c\rangle, \tag{16}$$

where Q is defined as the overlap of two F-center functions: $Q=\langle a_s|c_s\rangle$, etc. When the explicit forms [Eq. (3)] for the F-center wave functions are introduced, the following expression for $\langle a|\sum_k\xi_k l_k{}^z|c\rangle$ is obtained:

$$\begin{aligned}\langle a|\sum_k\xi_k l_k{}^z|c\rangle&=\langle a_s|\sum_k\xi_k l_k{}^z|c_s\rangle\\&\quad-\langle a_s|\sum_k\xi_k l_k{}^z|\sum_{k',\alpha'}\Omega_{ck'\alpha'}\phi_{k'\alpha'}\rangle\\&\quad-\langle\sum_{k'',\alpha''}\Omega_{ak''\alpha''}\phi_{k''\alpha''}|\sum_k\xi_k l_k{}^z|c_s\rangle\\&\quad+\langle\sum_{k'',\alpha''}\Omega_{ak''\alpha''}\phi_{k''\alpha''}|\sum_k\xi_k l_k{}^z|\\&\qquad\times\sum_{k',\alpha'}\Omega_{ck'\alpha'}\phi_{k'\alpha'}\rangle.\end{aligned} \tag{17}$$

As in the calculation of the spin-orbit splitting of the excited states of the F center,[9] the first three terms are expected to yield contributions amounting to roughly 10% of the total value, and will therefore be neglected. The last term is evaluated using the method introduced by Adrian.[12] As a result of the symmetry of the "unrelaxed" model, only one ion contributes to this matrix element. This is the Cl^- ion which corresponds to the reflection of F-center B (see Fig. 1) in the plane passing through AC and perpendicular to the plane of the R center. The remaining ions give contributions cancelling in pairs. The following expression is then obtained for λ_E

$$\lambda_E=3(Q^2+2Q)\beta^2Z(Cl^-)\left\langle\frac{1}{r^3}\right\rangle_{Cl^-}, \tag{18}$$

where $Q=0.385$, $Z(Cl^-)=14$ is an effective atomic number for Cl^-,[13] and the value for $\langle 1/r^3\rangle_{Cl^-}$, 1.6×10^{23} cm^{-3}, is obtained from ENDOR data of Feher.[14] When the small polar admixtures[15,16] are considered, the pure Heitler-London value is reduced by 0.6 cm^{-1}, and one obtains

$$\lambda_E=2.1\ cm^{-1}.$$

---

[12] F. J. Adrian, Phys. Rev. **107**, 488 (1957).
[13] R. G. Barnes and W. V. Smith, Phys. Rev. **93**, 95 (1954).
[14] G. Feher, Phys. Rev. **105**, 1122 (1957).
[15] J. O. Hirschfelder, J. Chem. Phys. **6**, 795 (1938).
[16] D. C. Krupka, thesis, Cornell University, 1966 (unpublished).

(b) *Calculation of* g_{OE}

Using only Heitler-London wave functions in (10), g_{OE} is given by

$$g_{OE}=-3\sqrt{3}i\langle a|l_0{}^z|c\rangle. \tag{19}$$

For the matrix element $\langle a|l_0{}^z|c\rangle$ one obtains

$$\langle a|l_0{}^z|c\rangle=\langle a_s|l_0{}^z|c_s\rangle-2\langle a_s|l_0{}^z|\sum_{k,\alpha}\Omega_{ck\alpha}\phi_{ka}\rangle + \langle\sum_{k,\alpha}\Omega_{ak\alpha}\phi_{k\alpha}|l_0{}^z|\sum_{k',\alpha'}\Omega_{ak'\alpha'}\phi_{k'\alpha'}\rangle. \tag{20}$$

Here the following fact, which can be readily demonstrated, has been used

$$\langle a_s|l_0{}^z|\sum_{k,\alpha}\Omega_{ck\alpha}\phi_{k\alpha}\rangle=\langle\sum_{k,\alpha}\Omega_{ak\alpha}\phi_{k\alpha}|l_0{}^z|c_s\rangle. \tag{21}$$

The three terms will now be considered individually. Table I summarizes the results.

(i) $\langle a_s|l_0{}^z|c_s\rangle$. Now

$$l_0{}^z=(\mathbf{d}_{0k}\times\mathbf{p})^z+l_k{}^z, \tag{22}$$

where $\mathbf{d}_{0k}$ is the vector from the center of the system to the point k with components X_{0k}, Y_{0k}, and Z_{0k}. For ease in computation, the point k is chosen to be the center of F center C since $l_0{}^z|c_s\rangle=0$. Thus

$$\langle a_s|l_0{}^z|c_s\rangle=i\langle a_s|Y_{0C}\frac{\partial}{\partial x}-X_{0C}\frac{\partial}{\partial y}|c_s\rangle. \tag{23}$$

Gourary and Adrian[17] type-I wave functions are employed for a_s and c_s, and the overlaps $\langle a_s|(\partial/\partial X)c_s\rangle$ are computed using a spheroidal coordinate system.[18] The calculation yields

$$\langle a_s|l_0{}^z|c_s\rangle=-0.177i.$$

(ii) $-2\langle a_s|l_0{}^z|\sum_{k,\alpha}\Omega_{ck\alpha}\phi_{k\alpha}\rangle$. This matrix element may be written

$$-2\langle a_s|\sum_k l_k{}^z|\sum_\alpha\Omega_{ck\alpha}\phi_{k\alpha}\rangle -2\langle a_s|\sum_k(\mathbf{d}_{0k}\times\mathbf{p})^z|\sum_\alpha\Omega_{ck\alpha}\phi_{k\alpha}\rangle.$$

Evaluation of the first term proceeds in a manner analogous to that used in computing the spin-orbit matrix elements. The second term is more difficult. Analytic self-consistent-field wave functions (simple basis set) calculated by Bagus[19] are employed and only $3s$ and $3p$ orbitals are considered since the contributions from other shells are negligible. The two-center overlap integrals were calculated using the method of Gourary and Adrian[17,20] whenever applicable. Otherwise standard methods[18] were employed. Contributions are considered only from ions which are within $\sqrt{2}\times$ (nearest-neighbor distance from one of the F centers appearing in the matrix element) and no farther than $(\sqrt{6})\times$ (nearest-neighbor distance from the other). Since the calculation of these terms depends sensitively on geometry,[21] the disparity of the contributions from the K^+ and Cl^- shells indicated in Table I is not surprising.

(iii) $\langle\sum_{k,\alpha}\Omega_{ak\alpha}\phi_{k\alpha}|l_0{}^z|\sum_{k',\alpha'}\Omega_{ak'\alpha'}\phi_{k'\alpha'}\rangle$. Only contributions arising from orbitals centered on the same ion, k, are considered, yielding

$$\langle\sum_\alpha\Omega_{ak\alpha}\phi_{k\alpha}|\sum_k(\mathbf{d}_{0k}\times\mathbf{p})^z|\sum_{\alpha'}\Omega_{ck\alpha'}\phi_{k\alpha'}\rangle + \langle\sum_\alpha\Omega_{ak\alpha}|\sum_k l_k{}^z|\sum_{\alpha'}\Omega_{ck\alpha'}\phi_{k\alpha'}\rangle.$$

Evaluation of these terms proceeds in a manner analogous to that discussed in (ii) above.

Using the data summarized in Table I, and taking $\mathcal{E}_x$ and $\mathcal{E}_y$ to be Heitler-London states, g_{OE} is given by

$$g_{OE}(H\text{-}L)=0.30.$$

Taking into account polar admixtures one obtains

$$g_{OE}=0.48.$$

D. Numerical Expressions

When the inequality $\Delta(\sigma)\gg\lambda_R$ holds, (13) reduces to

$$\delta g_{||}=2\lambda_E g_{OE}\left[\frac{f_{11}{}^2}{\Delta(\sigma)}+\sum_{p=2}^{\infty}\frac{(f_{1p})^2}{E_{yp\frac{1}{2}}-E_{x1\frac{1}{2}}}\right]. \tag{24}$$

Using numerical values for the LHOPS problem[22] and ignoring the stress dependence in the second energy denominator one obtains, for the case $k^2=2.0$ with $\lambda_E=2.1$ cm^{-1}, $g_{OE}=0.48$

$$\delta g_{||}=0.017/\sigma+0.0067,$$

while for $k^2=5.0$

$$\delta g_{||}=0.00047/\sigma+0.0032.$$

In evaluating the above, ω_E has been taken to be 80

TABLE I. Summary of the contributions to the matrix element $\langle a|l_0{}^z|c\rangle$.

	Vacancy-vacancy term	Vacancy-ion term K^+ shell	Vacancy-ion term Cl^- shell	Ion-ion term K^+ shell	Ion-ion term Cl^- shell	Total
$\langle a\|l_0{}^z\|c\rangle$	$-0.177i$	$+0.001i$	$+0.040i$	$-0.125i$	$-0.131i$	$-0.39i$

[17] B. S. Gourary and F. J. Adrian, in *Solid State Physics*, edited by F. Seitz and D. Turnbull (Academic Press Inc., New York, 1960), Vol. 10, p. 128.

[18] C. J. Ballhausen, *Introduction to Ligand Field Theory* (McGraw-Hill Book Company, Inc., New York, 1962), p. 174.

[19] P. S. Bagus, Argonne National Laboratory Report No. ANL-6959, 1964 (unpublished).

[20] The authors are grateful to Dr. F. J. Adrian for making available numbers required in the calculation of some of the overlap integrals.

[21] J. C. Slater and G. F. Koster, Phys. Rev. **94**, 1498 (1954).

[22] The authors are greatly indebted to Professor H. C. Longuet-Higgins for providing numerical values for the eigenvalues and eigenvalues of the LHOPS problem.

cm^{-1} as estimated from the optical experiments in I, and the [110] stress σ is to be expressed in kg/mm^2.

Two important features of the above results should be pointed out. The first is that δg_{II} is *positive*, the positive shift arising from the fact that the spin-orbit interaction results from currents about the nuclei which have angular momentum opposite in sense to that of the center as a whole. Reference 9 contains drawings which illustrate this effect for the excited state of the F center. The sign of the g shift is in agreement with the observed shift described in the Introduction. The second feature which merits comment is the relative magnitude of the two contributions as a function of k^2. A measurement of g as a function of stress is expected to yield information on the strength of the Jahn-Teller coupling. A limit for k^2 was obtained in I where it was shown that $k^2 \lesssim 7$.

E. Results

The observed line shapes with H_0 in the $[1\bar{1}1]$ direction for increasing applied [110] stress are shown in Fig. 3. The large signal arises primarily from F centers and no R center signal is observed for zero applied stress. As the stress is increased, the line narrows and shifts toward the F-center resonance which does not shift with stress. The linewidth is approximately 100 G at an applied stress of 0.3 kg/mm^2 and narrows to about 50 G at high stress where the broadening is presumably due to hyperfine interaction. (The term "F-center resonance" will be used here to refer to the signal in the region of the F-center resonance. This signal includes contributions from R centers as well as the saturated F-center signal.) It is important to note that the R and F signals do not add linearly. This fact is interpreted as resulting from cross relaxation[23] of the

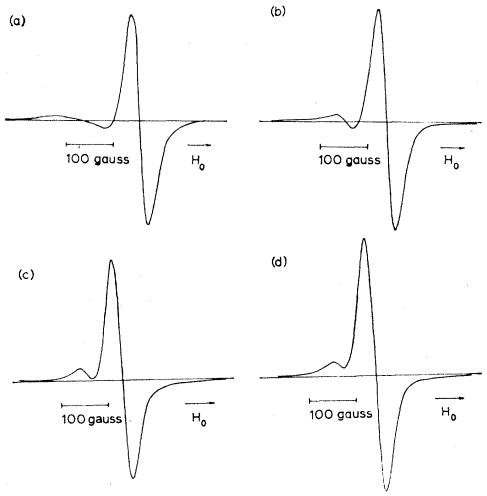

FIG. 3. Line shapes for different applied stresses. The large signal arises primarily from the F-center resonance. $T=2.2$°K. (a) 0.3 kg/mm^2; (b) 0.83 kg/mm^2; (c) 1.8 kg/mm^2; (d) 2.6 kg/mm^2.

[23] N. Bloembergen, S. Shapiro, P. S. Pershan, and J. O. Artman, Phys. Rev. **114**, 445 (1959).

F center through the more rapidly relaxing R centers. This mechanism, coupled with a rapid spectral diffusion rate[24] in the F center which serves to return the signal to its "normal" shape will help to explain why one does not observe signals from R centers with $[\bar{1}11]$, [111], and $[11\bar{1}]$ symmetry axes when the magnetic field is along the $[1\bar{1}1]$ direction.

The partial resolution of the R resonance together with the mechanisms described above makes an accurate determination of the g extremely difficult. This difficulty is compounded at low stresses where the line shape is asymmetric. Changes in g due to applied stress or change in magnetic field orientation may be measured somewhat more accurately. In general, the g value was estimated as follows: When the g was sufficiently large to permit a "zero-crossing" to be observed [see Fig. 3(a)] the g was determined from the point at which the derivative curve passed through zero. For larger applied stresses as in Figs. 3(b) and 3(c), the g was estimated by reconstructing the low-field tail of the F-center line to reproduce the high-field tail. In addition, tracings were made of the line shapes at different stresses and relative shifts estimated.

Figure 4(a) is a plot of δg_{II} as a function of the reciprocal of the applied stress, $1/\sigma_{app}$, for five different crystals. For annealed crystals the data exhibit a definite negative curvature, and reproduce reasonably well from sample to sample when one takes into account the large errors arising from the difficulty in estimating the g. These data are used to determine k^2 by fitting to Eq. (24). This involves the tacit assumption that $\Delta(\sigma=1 \text{ kg/mm}^2) \gg \lambda_R$. The validity of this assumption is considered later in this section. Since the results of the optical experiments suggest random internal stresses of the order of 1 kg/mm^2, the total stress σ is written as $\sigma=\sigma_{app}+\sigma_0$ where σ_0 is the random internal stress, and is to be determined by fitting.

The curves of Fig. 4(a) are plots of Eq. (24) for $k^2=2.0$ with values of $\sigma_0=0.5$, 1.0, 1.5 kg/mm^2 fitted to a value of $\delta g_{II}=0.038$ at $1/\sigma_{app}=0.5$ mm^2/kg.

It is clear that one cannot obtain a fit for $k^2=2.0$ at any reasonable value of σ_0. Fits are obtained, however, for $k^2=3.0$ as indicated in Fig. 4(b). It appears from this figure that the best fit is for $k^2=3.0$ and $\sigma_0=1$ kg/mm^2. Additional plots, not shown, indicate that the two parameters of interest are

$$k^2=3.0\pm0.5$$

and $\sigma_0=1.0\pm0.3$ kg/mm^2.

No systematic study was carried out on the effects of annealing. It can be seen that the unannealed sample 11 exhibits a markedly different behavior. It is felt that this crystal was badly strained before the run. There is evidence for this as the resonance becomes observable at a lower value of applied stress than for

[24] A. M. Portis, Phys. Rev. **104**, 584 (1956).

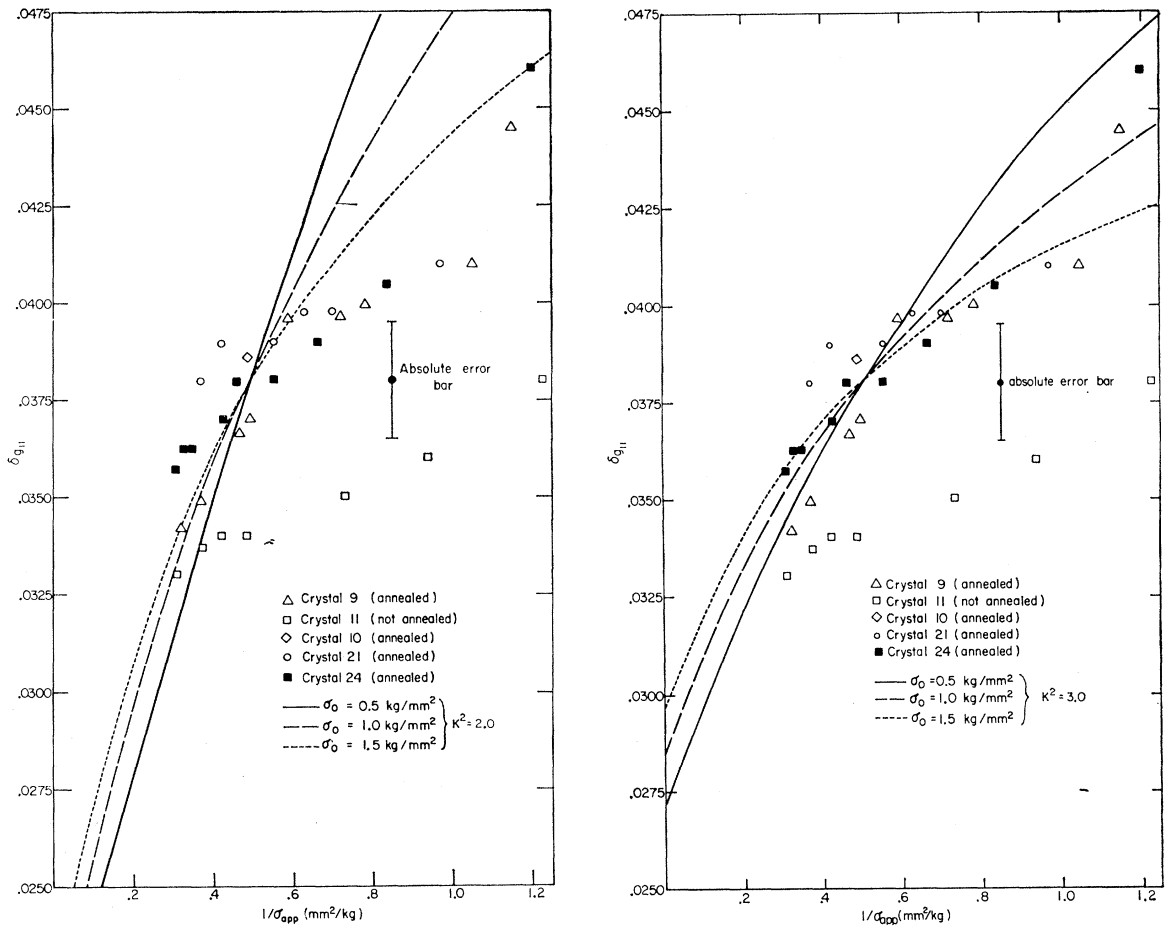

FIG. 4. (a) $\delta g_{||}$ plotted as a function of $1/\sigma_{app}$. Data taken at 2.2°K. The curves are attempts to fit the data with $k^2=2.0$ and selected values of σ_0, the random internal stress. (b) $\delta g_{||}$ plotted as a function of $1/\sigma_{app}$. Data taken at 2.2°K. The curves are attempts to fit the data with $k^2=3.0$ and selected values of σ_0, the random internal stress.

the annealed crystals. An attempt to fit the data for sample 11 using $\sigma_0=2$ kg/mm² was not successful.

Having determined the value of k^2, one deduces the following value for the product $g_{OE}\lambda_E$:

$$(g_{OE}\lambda_E)_{\text{deduced}}=5.3_{-0.6}^{+1.1}\ \text{cm}^{-1}.$$

This is to be compared with the theoretically determined value for this product of 1.0 cm^{-1}. The discrepancy may be partly accounted for by small changes in R/a_0, where R is the separation between the vacancies making up the R center and a_0 is the F-center "Bohr" radius.[17] A 10% decrease in R/a_0 which could quite conceivably arise from ionic relaxation leads to an increase in g_{OE} of about a factor of 3. The ionic relaxation also removes the cancellation in pairs of the contributions of various ions to λ_E which is inherent in the "unrelaxed" model, giving further uncertainty in λ_E.

The value of $g_{OE}\lambda_E$ deduced from experiment is certainly more reliable than the calculated value. Hence, in the following discussion the parameters g_{OE} and λ_E will be assumed larger than the calculated values by a factor of 2.3 chosen to give the experimental value for the product $g_{OE}\lambda_E$. Thus

$$g_{OE_{\text{deduced}}}=1.1,$$
$$\lambda_{E_{\text{deduced}}}=4.8\ \text{cm}^{-1}.$$

The adjustment is shared equally between the two parameters since, though the calculation of g_{OE} is more reliable than that of λ_E for a given R/a_0, it is also more sensitive to the assumed value of R/a_0 and hence to the effects of ionic displacements. Note that the value of $g_{OE}\lambda_E$ deduced from experiment is certainly more reliable than either of the values given above for the constants separately.

Figure 5 is a plot of the g value for a $[1\bar{1}1]R$ center as a function of orientation for sample 24A at an applied stress of 1.55 kg/mm². The solid lines are determined from

$$g_{\text{eff}}=(g_{11}^2\cos^2\theta+g_\perp^2\sin^2\theta)^{1/2},\qquad(25)$$

where θ is the angle between H_0 and the symmetry axis. The value for $g_{\parallel}$ is determined by fitting near $\theta=0$ for the $[1\bar{1}1]R$ centers, while $g_{\perp}$ is calculated using the deduced values of λ_E and g_{OE} with the reduction factor f_{11} appropriate for $k^2=3.0$ ($f_{11}=0.075$).[22] Using $\Delta(\sigma_{app}+\sigma_0)$ with $\sigma_0=1$ kg/mm^2 one obtains $g_{\perp}=1.997$. Since data may be obtained only over a severely limited range of angles, the plot does not constitute a sensitive measure of $g_{\perp}$. The agreement is reasonable although there appears to be a tendency for the points to move toward $g=2$ faster than predicted.

There remain two important experimental results to be explained: (1) the lack of a resonance signal at zero stress, and (2) the lack of an observable signal at $g_{\perp}$ at all values of stress. These results are explained below in terms of the effects of random internal stresses.

The line at $g_{\parallel}$ is considered first. As a result of the random stresses, one expects, at zero applied stress, a distribution of $g_{\parallel}(\sigma)$ values with σ ranging from 0 to about 1 kg/mm^2. Using the deduced values of g_{OE} and λ_E, this yields a spread of 235 G. If to this value is added the residual linewidth one obtains at zero applied stress a linewidth of 285 G. Some idea of the limits of detectability may be gained from Fig. 3(a). In this figure, for $\sigma_{app}=0.3$ kg/mm^2, the linewidth is about 100 G and the signal-to-noise ratio 8:1. Since the signal height is proportional to $(1/\Delta H)^2$, a linewidth of 285 G implies an undetectable signal in view of the signal-to-noise ratio. The above discussion has not taken into account the fact that the signal at $g_{\parallel}$ is proportional to $[g_{\perp}(\sigma)]^2$. Since $g_{\perp}=0$ for $\sigma=0$, the signal from R centers at sites with very low random stress will be correspondingly small.

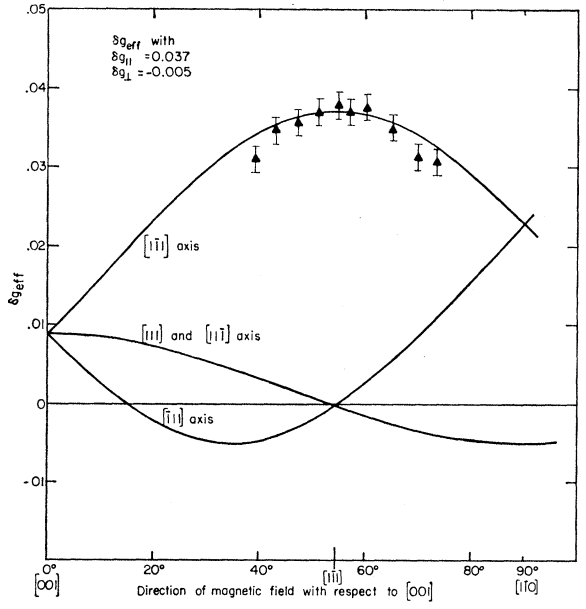

FIG. 5. δg_{eff} as a function of orientation for sample 24A. $\sigma_{app}=1.6$ kg/mm^2. $T=2.1$°K.

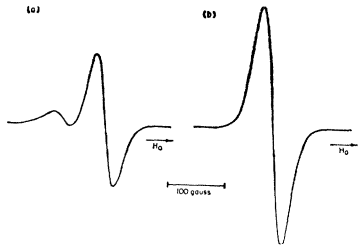

FIG. 6. Signals observed for identical rf powers at $\sigma_{app}=1.9$ kg/mm^2. (a) $H_0\|[1\bar{1}1]$; (b) $H_0\|[1\bar{1}0]$. The audio gain in (a) is larger by a factor of 1.12. The difference in signal size is due primarily to a difference in filling factor.

The lack at all stresses of an observable signal at $g_{\perp}$ is explained in a manner similar to the foregoing. Consider Fig. 6 which indicates the observed signals with H_0 parallel to the $[1\bar{1}1]$ and $[1\bar{1}0]$ direction for $\sigma_{app}=1.9$ kg/mm^2. It is seen that for the latter orientation the R signal has disappeared entirely in the F-center resonance. The rapid spectral diffusion within the F center has restored the signal to its "normal" shape. In fact, it is observed that the R-center signal disappears inside the F resonance for $\delta g_{eff}\leq 0.025$. Thus one does not expect to see the line at $g_{\perp}$ for $|\delta g_{\perp}|\leq 0.025$. Such a value corresponds to a total stress of 1 kg/mm^2. Since sites with zero stress have $g_{\perp}=0$, the $g_{\perp}$ line is spread over some 3000 G for small applied stress. At moderate applied stresses the line is stabilized under the resonance arising from F centers and no evidence for its presence is seen. One concludes, therefore, that strain broadening exists and is, in all likelihood, the reason for the absence of a signal at small applied stress.

In analyzing Fig. 4, the assumption was made that λ_R was much smaller than the stress splitting $\Delta(\sigma=1$ kg/mm$^2)=2.2$ cm^{-1}. Since λ_R is found to be 0.36 cm^{-1} the data have been interpreted in a self-consistent fashion. The negative curvature of Fig. 4 could be accounted for, also, on the assumption that $\lambda_R\approx\Delta(\sigma=1$ kg/mm^2). In this case, with the smaller g_{OR} required by the experimentally determined value of λ_R g_{OR}, one would be hard pressed to explain the lack of signal at $\delta g_{\parallel}$ for small stress. In addition, one should expect to observe the signal at $g_{\perp}$ unless ionic relaxation contrives to yield just the right $\delta g_{\perp}$ to place the signal under the F resonance. This is considered rather unlikely.

An unsuccessful attempt was made to observe all four R-center resonances merely by using sufficiently large rf power to "saturate out" the F centers. The signal observed at these high powers was highly distorted and indicated that the various mechanisms involved: saturation, cross relaxation, and spectral diffusion combine to produce very complex passage effects.[25,26] No serious attempt was made to understand

[25] M. Weger, Bell System Tech. J. 39, 1013 (1960).
[26] A. M. Portis, Technical Note No. 1, Sarah Mellon Scaife Radiation laboratory, University of Pittsburgh, 1955 (unpublished).

these. Suffice it to say that in no instance was there any indication that one had resolved the R resonances.

IV. SPIN-RELAXATION PROCESSES

A. Theory

In calculating spin-relaxation processes, use is made of the effective-strain Hamiltonian introduced in I, and the strain is expanded in terms of phonon creation and annihilation operators.

(a) T_1 Processes

A consideration of the energy levels for the R center with the dc magnetic field H_0 along a $\langle 111\rangle$ symmetry axis leads to the conclusion that there will be no spin-lattice relaxation in the absence of an additional perturbation such as hyperfine interaction. A finite spin-lattice relaxation rate may be calculated, however, when H_0 is not parallel to the defect symmetry axis. Under the assumption that static strain is the dominant term in the effective Hamiltonian, the following expression for a direct relaxation rate is obtained when the magnetic field is rotated through an angle θ in the xz plane (see Fig. 1):

$$\left(\frac{1}{T_1}\right)_{\text{direct}}=\frac{1}{32\pi}\left\{\frac{\beta HB\omega\lambda_R\sin\theta}{\hbar\Delta^2}\right\}^2\frac{kT}{\rho v^5}, \tag{26}$$

where B is a stress coupling coefficient obtained in I; $B=0.4\times10^{-12}$ erg, ω is the transition frequency, ρ is the density of the crystal, v is the velocity of sound ($v=2\times10^5$ cm sec^{-1}), k is Boltzmann's constant, and T is the temperature. For an applied stress of 2 kg/mm^2 this yields a value

$$(1/T_1)_{\text{direct}}\approx4\times10^3\sin^2\theta\ T\ \text{sec}^{-1}.$$

One may also obtain an expression for an Orbach process[27] in which the relaxation proceeds by way of the strain-split state lying at approximately $\Delta(\sigma)$ above the lowest Kramers doublet. In this case one obtains, for $\Delta\gg kT$,

$$\left(\frac{1}{T_1}\right)_{\text{Orbach}}\approx\frac{B^2\lambda_R^2\sin^2\theta\Delta e^{-\Delta/kT}}{2\rho v^5\hbar^4}. \tag{27}$$

For an applied stress of 2 kg/mm^2 at 2°K,

$$(1/T_1)_{\text{Orbach}}\approx2\times10^6\sin^2\theta\ \text{sec}^{-1}.$$

The angular dependence of the spin-lattice relaxation time suggests a possible relaxation mechanism when H_0 is normally along the defect axis: A possible misalignment of the crystal of about 1° would result in a negligible direct rate but a reasonable value for the Orbach rate.

Spin-lattice relaxation rates have also been calculated[16] taking into account the hyperfine interaction. For H_0 along the defect axis these relaxation rates are negligible compared to those arising from the misalignment described above.

Any realistic discussion of spin-lattice relaxation of the line at $g_{\parallel}$ must take into account the possibility of cross relaxation of that line with the other three (see Fig. 5) which have relatively large values of $\sin\theta$. No estimate of this process has been attempted, however.

(b) T_2 Processes

For small stresses when the separation between the ground state and the strain-split state, $[\Delta^2+\lambda_R^2]^{1/2}$, is of the order of kT, a rapid T_2 process exists. Since the g of the strain-split state differs from that of the ground state, excitation between this pair of Kramers doublets will yield a T_2 mechanism. The calculation is straightforward and yields

$$\frac{1}{T_2}\approx\frac{B^2(\Delta^2+\lambda_R^2)^{3/2}n[(\Delta^2+\lambda_R^2)^{1/2}]}{8\pi\rho v^5\hbar^4}$$
$$\approx10^8(\Delta^2+\lambda_R^2)^{3/2}n[(\Delta^2+\lambda_R^2)^{1/2}]\ \text{sec}^{-1} \tag{28}$$

using the same values for the parameters as in the T_1 calculation. Here $n[(\Delta^2+\lambda_R^2)^{1/2}]$ is the phonon occupation number at $(\Delta^2+\lambda_R^2)^{1/2}$ and the energy is to be expressed in cm^{-1}.

B. Results and Discussion

Information concerning the spin-lattice relaxation time T_1 is obtained in these experiments solely from saturation plots. The quantity $(T_1T_2)^{1/2}$ is determined from the value of the rf field at the knee of the curve as in Figs. 7 and 8. Measurements have been made to obtain some understanding of T_1 as a function of stress, temperature, and orientation. The primary motivation throughout has been to establish whether or not the broadening of the R line at low stress is due to T_1 as suggested in Ref. 1.

(a) Stress Dependence

Since the line is very broad at low stress it is not possible to determine reliably whether or not there is saturation. One turns, therefore, to data at higher stresses in an attempt to infer from these the low stress behavior. Figure 7 indicates saturation plots for three different applied stresses at 2.1°K. There is a definite increase in T_1T_2 as the stress is increased. The data for sample 21A indicate that T_1T_2 reproduces reasonably well from sample to sample, and it is assumed that the data presented in Fig. 7 for sample 25A may be applied to the analysis of the data from all other crystals.

The data of Figs. 3 and 7 are now used in an argument to eliminate T_1 as a source of line broadening. In Fig. 3, showing the line shapes as a function of stress at 2°K, it is seen that the linewidth is 100 G at $\sigma_{\text{app}}\approx0.8$ kg/mm^2 ($\sigma=\sigma_{\text{app}}+\sigma_0\approx1.8$ kg/mm^2). Taking the resi-

[27] R. Orbach, Proc. Phys. Soc. (London) **A77**, 821 (1961).

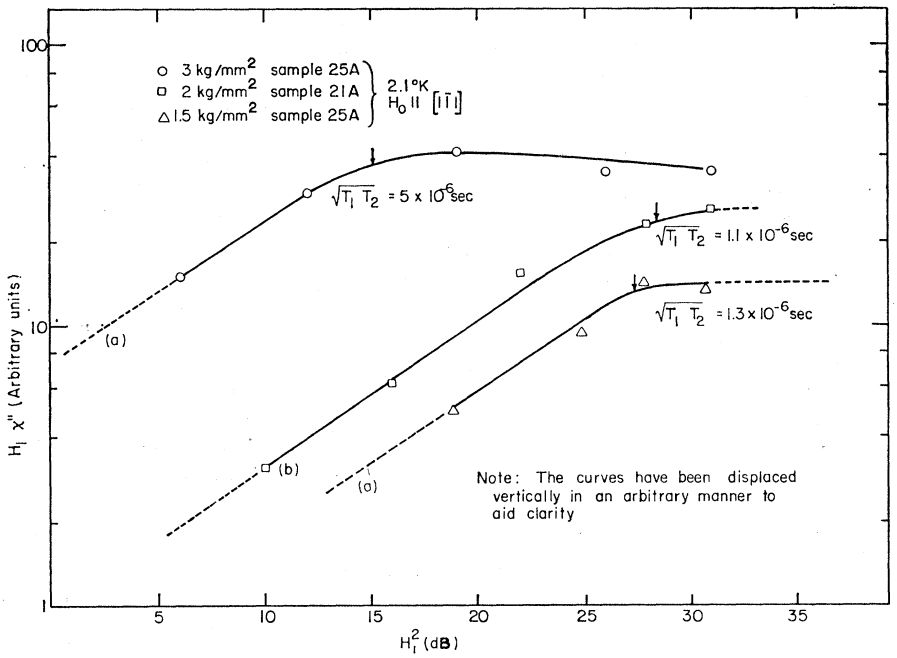

FIG. 7. Saturation plots taken at 2.1°K with $H_0 \| [1\bar{1}1]$ at different applied stresses. (a) sample 25A, $\sigma_{app}=3$ kg/mm²; (b) sample 21A, $\sigma_{app}=2$ kg/mm²; (c) sample 25A, $\sigma_{app}=1.5$ kg/mm².

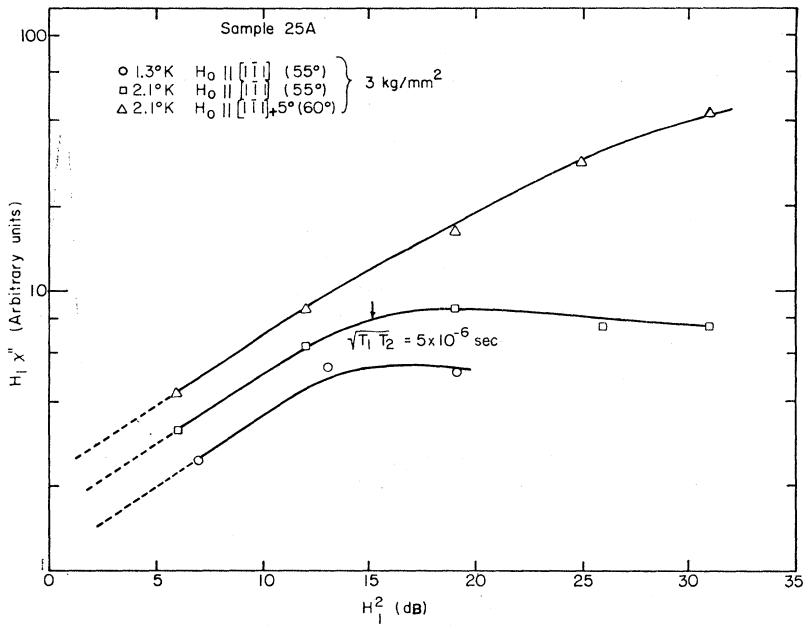

FIG. 8. Saturation plots taken with $\sigma_{app}=3$ kg/mm². (a) $T=2.1$°K, $H_0\|[1\bar{1}1]+5°$ (60° in Fig. 5); (b) $T=2.1$°K, $H_0\|[1\bar{1}1]$ (55° in Fig. 5); (c) $T=1.3$°K, $H_0\|[1\bar{1}1]$.

dual line breadth to be 50 G, there thus remains 50 G to be accounted for.[28] If spin-lattice relaxation broadening is invoked to explain the additional width, one requires $T_1 \approx 10^{-9}$ sec at $\sigma=1.8$ kg/mm². Now Fig. 7 indicates that the shortest T_1 possible (obtained by taking $T_1=T_2$) for $\sigma_{app}=1.5$ kg/mm² ($\sigma \approx 2.5$ kg/mm²) is 1.3×10^{-6} sec. Thus, in order to explain the broadening, one requires T_1 to decrease by a factor of 10^3 for a change in σ of a factor of 1.8/2.5. Such a sensitivity of T_1 on stress is not predicted in the calculations, and would require that the line disappears in going from $\sigma_{app}=0.8$ kg/mm² to $\sigma_{app}=0.3$ kg/mm². This is not observed experimentally as witnessed by Fig. 3. T_1 as a source of line broadening is thus eliminated.

Although the possibility of T_2 broadening may not be dismissed as easily, the process described by Eq. (28) which must be a leading contribution to T_2 can be eliminated. The energy dependence in Eq. (28) indi-

[28] Note that the following argument would be even stronger if the linewidths were assumed to be as $W^2(\text{total})=\sum_i (W_i)^2$.

cates that the process will have a maximum for $[\Delta^2+\lambda_R{}^2]^{1/2}\approx 4$ cm^{-1} at 2°K, corresponding to a total stress of approximately 2 kg/mm^2. Thus this process will not yield line broadening at low stress.

(b) *Temperature Dependence*

Figure 8 shows saturation plots for sample 25A at 1.3 and 2°K. It can be seen that the temperature dependence of T_1T_2 is very weak indeed with $(T_1T_2)^{1/2}$ approximately equal to 5×10^{-6} sec for $\sigma_{\rm app}=3$ kg/mm^2. The same weak temperature dependence also appeared in the only other sample studied, which yielded $(T_1T_2)^{1/2}=2.5\times10^{-6}$ sec at the same stress. It was reported in Ref. 1 that no resonance was observed at 4.2°K, and this was taken as further evidence for T_1 broadening by an Orbach process. A further search was made for the resonance at this temperature and the signal was observed. No signal was seen, however, at 77°K. Since the signal-to-noise ratio at 4.2°K was already only about 4:1, no attempt was made to look for it between 4.2 and 77°K.

(c) *Angular Dependence*

Figure 8 indicates a saturation plot for sample 25A taken with the static field 5° away from the $[1\bar{1}1]$ direction. The plot is strikingly different from plots taken with H_0 parallel to the $[1\bar{1}1]$ direction and suggests a much shorter T_1. Thus the result is in qualitative agreement with calculation. No systematic study was carried out of the angular dependence of the saturation plots.

The experimental results rule out the Orbach process, and suggest, instead, a direct one ($1/T_1\propto T$) with strong angular dependence. In addition, the possibility of cross relaxation of the line at $g_{\parallel}$ through the lines near $g_{\perp}$ should not be overlooked. Proper elucidation is once again hampered by the difficulty in properly resolving the R resonance.

V. INFLUENCE OF THE R CENTER ON THE SPIN-LATTICE RELAXATION TIME T_{1F} OF THE F CENTER

A. Background

The spin-lattice relaxation time T_{1F}, for isolated F centers ($N_F\approx10^{16}$ cm^{-3}) in KCl has been studied by Feldman, Warren, and Castle.[29] The relaxation proceeds by way of the modulation of the hyperfine interaction yielding a value for T_{1F} at 2°K of approximately 5×10^4 sec at a field of 3.2 kG; the relaxation rate is increased by high F concentrations and by exposure to light.[30] "Extrinsic" behavior such as described above had been observed earlier by a number of authors[31–33] who found that such behavior could not be correlated with the presence of aggregate centers. In particular, Warren, Feldman, and Castle[30] carried out an experiment in which uniaxial stress was applied to the crystal and a corresponding change was sought in T_{1F}. These authors argued, on the basis of Ref. 1, that stress increased T_{1R}, and this, in turn should increase T_{1F} if the F center cross relaxes through the R. No stress-dependent change in T_{1F} was observed.

The results of the two preceding sections indicate that the method described above is not a sensitive way of testing for effects of the R center. Stress does increase T_{1R} but at the same time increases F-R overlap. A more fruitful approach is to use the g anisotropy under conditions of large applied stress and to look for an anisotropic T_{1F}.

B. Results and Discussion

(a) *High-Concentration Experiments*

Studies were made at high and low concentrations. The high concentration experiments ($N_F\approx10^{17}$ cm^{-3}, $N_R\approx5\times10^{15}$ cm^{-3}) are considered first. From saturation measurements at these concentrations, a value of $(T_1T_2)_F{}^{1/2}$ of 10^{-4} sec was deduced (determined from the value of H_1 at which saturation just begins to set in).

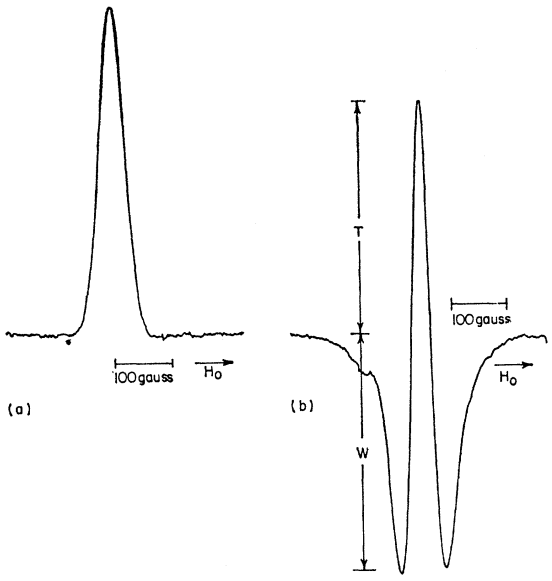

FIG. 9. Sample 17 (a) $\chi'(90°)$, (b) $\chi'(0°)$. Signals observed with $H_0\|[1\bar{1}1]$ at $T=2.2$°K under the following conditions: $H_1\approx1/20$ G, $dH_0/dt=100$ G min^{-1}, $H_m=9.5$ G, $\sigma_{\rm app}=3$ kg/mm^2, $\omega_m=220$ r/sec, $N_R/N_F\approx1/20$. The bump on the low-field side of $\chi'(0°)$ may be due to an R center which should be down in intensity by a factor of about 1/80.

[29] D. W. Feldman, R. W. Warren, and J. G. Castle, Jr., Phys. Rev. **135**, A470 (1964).
[30] R. W. Warren, D. W. Feldman, and J. G. Castle, Jr., Phys. Rev. **136**, A1347 (1964).
[31] P. R. Moran, S. H. Christensen, and R. H. Silsbee, Phys. Rev. **124**, 442 (1961).
[32] W. D. Ohlsen and D. F. Holcomb, Phys. Rev. **126**, 1953 (1962).
[33] M. Schwoerer and H. C. Wolf, Z. Physik **175**, 457 (1963).

Such a value suggested that it might be possible to carry out the experiments outlined above by using the method first employed by Portis[34] to measure T_{1F} at room temperature. Under the assumption that $T_1=T_2$, $\omega_m T_1 \ll 1$ (where ω_m is the modulation frequency, and $\omega_m H_m T_1 < H_1$ (where $2H_1$ is the peak transverse rf field and H_m is the peak modulation field), T_1 is given by[34]

$$T_1 \approx 0.062 H_1 \chi_0'(90°)/\omega_m \chi_0'(0°), \qquad (29)$$

where χ_0' is the real part of the rf susceptibility measured at the center of the line. The quantity in brackets refers to the phase angle between the modulation signal and the lock-in reference signal.

Typical observed signals are shown in Fig. 9. Qualitatively they have the appearance predicted.[26,34] The $\chi'(90°)$ signal is Gaussian. For such a shape Streever and Bennett[35] point out that the ratio of "tail" to "wing" (T and W in Fig. 9) should be 3.5:1. Such a ratio, however, was never obtained. All attempts to explain the discrepancy on the basis of a combination of more complicated passage effects[24,25] have failed. The effects of spectral diffusion and cross relaxation probably complicate matters to the point where the situation is very difficult to analyze.

In spite of the difficulties encountered in attempting to explain the data in a straightforward manner, it still appeared fruitful to measure $\chi_0'(90°)/\chi_0'(0°)$ as a function of orientation in order to search for anisotropy. The results of this experiment are indicated in Fig. 10 where $\chi_0'(90°)/\chi_0'(0°)$ is plotted as a function of the direction of the magnetic field with respect to the crystal [001] direction. There is an obvious peaking for H_0 in the $[1\bar{1}1]$ direction suggesting a correlation with the presence of R centers which are barely discernible in Fig. 9. In addition, the ratio behaves qualitatively as it would if the simple theory[34] held, and T_{1F} were dependent on the overlap of the F and R resonances. That is, with H_0 in the $[1\bar{1}1]$ direction where the overlap is least, T_{1F} is expected to be longest, and at any given orientation T_{1F} should increase with applied stress. The main point is, however, that there is a definite orientational correlation of the relaxation behavior of the F center with the presence of R centers at these concentrations.

(b) *Low-Concentration Experiments*

Having established this behavior at high R concentrations, experiments were then carried out at low concentrations where T_{1F} had already been reduced by a factor of about 10^2 from its "intrinsic" value but where the R concentration was still extremely small. Since the method described above breaks down when $\omega_m T_1 \gg 1$, $\chi''(0°)$ was measured at rf powers sufficiently high to saturate to the point of somewhat distorting the signal. The motivation was to look for changes in the appearance of the signal as a function of orientation which could be correlated with the presence of R centers.

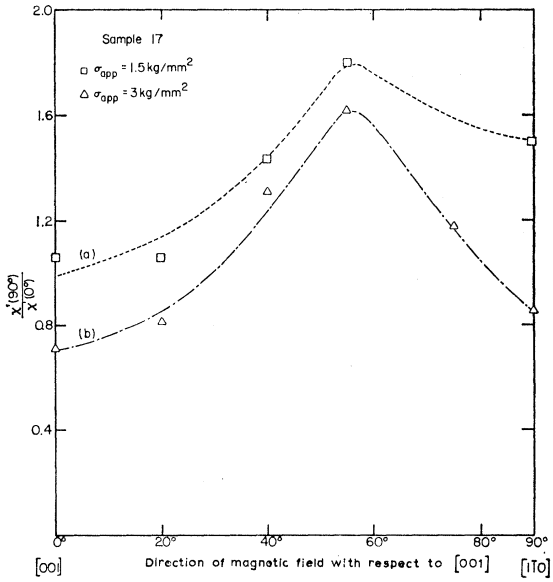

FIG. 10. $\chi'(90°)/\chi'(0°)$ as a function of the direction of the magnetic field H_0. Data taken on sample 17 at 2.2°K. (a) $\sigma_{app}=1.5$ kg/mm²; (b) $\sigma_{app}=3$ kg/mm².

The crystals were colored to yield an F-center density of approximately 5×10^{16} cm^{-3} and slightly bleached in the F band to produce an R concentration of about 1×10^{14} cm^{-3}. All subsequent handling was carried out in the dark. In order to make the experiments more sensitive, the R centers were selectively bleached[5] to yield a ratio N_R at $[1\bar{1}1]$ to N_R at any of the other three equivalent orientations of approximately 3:1.

The unsaturated line shapes were 40 ± 2 G broad and did not reproduce if reswept within 60 sec, suggesting that T_{1F} was of that magnitude. The measurements were carried out under the following conditions:

$$H_1 \approx 5\times10^{-5} \text{ G},$$
$$H_m = 9 \text{ G},$$
$$\omega_m = 220 \text{ rad sec}^{-1},$$
$$dH_0/dt = 50 \text{ G min}^{-1},$$
$$\sigma_{app} = 2 \text{ kg/mm}^2.$$

No evidence was found for any change in line shapes as a function of orientation which could be correlated with the presence of R centers. In addition, saturation measurements carried out on a crystal with $N_F \approx 5\times10^{16}$ cm^{-3} and $N_R \approx 2\times10^{14}$ cm^{-3} showed no orientational dependence for $\omega_m = 100$, 220, and 470 rad sec^{-1}.

These experiments thus lead to the following conclusions:

1. At ratios of F/R of approximately 20, R centers provide a significant cross-relaxation channel for F centers.

[34] A. M. Portis, Phys. Rev. **100**, 1219 (1955).
[35] R. L. Streever and L. H. Bennett, Phys. Rev. **131**, 2000 (1963).

2. The low-concentration experiments are in agreement with those of Warren, Feldman, and Castle[30] at similar concentrations. Thus, the drastic increase in the F relaxation rate brought about by bleaching F centers cannot be correlated with the presence of R centers. It is not possible to dismiss the R center altogether, as the rate limiting step in the F-center relaxation process[30,32] at these concentrations may not be the R-center relaxation.

VI. CONCLUSIONS

The main results of this study are summarized at the end of each section. The fact that the theoretical calculation of $\delta g_{\parallel}$ is a factor of about 5 smaller than the observed value is not too surprising in view of the sensitivity of the calculated number to the ratio R/a_0, and the rather primitive wave functions employed for the R center. As mentioned earlier, allowing for a reasonable 10% ionic relaxation would increase the calculated $\delta g_{\parallel}$ by a factor of about 3 at large stresses. In addition since the quantities λ_E and g_{OE} are much more sensitive to the wave functions than is the energy, the observed discrepancy is not too serious when one compares the calculated energy levels with those obtained from optical experiments as indicated in Fig. 4 of I.

It is unfortunate from the point of view of the ESR experiments that the Jahn-Teller effect is as strong as it is. The value for k^2 of 1.5 which yields an orbital reduction factor[22] f_{11} of about 0.19 would yield at large stresses a $\delta g_{\parallel}$ more than six times larger. This would permit a more complete study of the resonance.

ACKNOWLEDGMENTS

It is a pleasure to acknowledge many helpful conversations with L. L. Chase, Dr. D. L. Cowan, and Dr. V. Narayanamurti and the support of the Advanced Research Projects Agency through the Cornell Materials Science Center.

APPENDIX: CONTRIBUTIONS FROM EXCITED VIBRONIC STATES TO g^{zz} AND TO g^{xx} AND g^{yy}

A. g^{zz}

The contribution of the upper states is more easily calculated for the case where $\Delta(\sigma)\gg\lambda_R$ when one can take the vibronic ground state to be $\Psi_{x1\frac{1}{2}}$. Only states with electronic parts transforming as E need be considered. There are, in fact, two kinds of excited vibronic states. Those arising from excited electronic states and those arising from the ground electronic states. Consider first the latter. Using the fact that

$$\langle\Psi_{x1\frac{1}{2}}|\sum_i l_{0i}{}^z|\Psi_{ypl}\rangle=f_{1p}\langle\mathcal{E}_x|\sum_i l_{0i}{}^z|\mathcal{E}_y\rangle\delta_{l,\frac{1}{2}}, \quad (30)$$

which can be readily demonstrated using the formalism of LHOPS, the contribution to g^{zz} of the states in question is simply

$$\sum_{p=2}^{\infty}\frac{2\langle\Psi_{x1\frac{1}{2}}+|\mathcal{H}_{SO}|\Psi_{yp\frac{1}{2}}+\rangle\langle\Psi_{yp\frac{1}{2}}+|\mathcal{H}_{OZ}|\Psi_{x1\frac{1}{2}}+\rangle}{E_{yp\frac{1}{2}}-E_{x1\frac{1}{2}}}$$
$$=2\lambda_E g_{OE}\sum_{p=2}^{\infty}\frac{(f_{1p})^2}{E_{yp\frac{1}{2}}-E_{x1\frac{1}{2}}}. \quad (31)$$

The only other possible contribution comes from vibronic states derived from other electronic states transforming as E. The contribution will take the same form as above but will be negligible by comparison as the pertinent energy denominators will be larger by a factor of about 100 and the electronic matrix are expected to be of the same order of magnitude.

B. g^{xx} and g^{yy}

In calculating these terms one is interested in matrix elements of angular momentum and the spin-orbit interaction between the ground state and vibronic states derived from low-lying excited electronic states. One is thus ultimately interested in matrix elements of the type $\langle a|\sum_k \xi_k l_k{}^{x,y}|c\rangle$.

These matrix elements may be shown to be zero on the basis of the "unrelaxed" model of the R center. Except for one, the ions yield contributions canceling in pairs as in the calculation of $\langle a|\sum_k \xi_k l_k{}^z|c\rangle$. For the sole contributing ion k

$$\langle a|\xi_k l_x{}^{x,y}|c\rangle=0=\langle c|\xi_k l_k{}^{x,y}|b\rangle=\langle b|\xi_k l_k{}^{x,y}|a\rangle.$$

Hence the excited states do not contribute to g^{xx} and g^{yy}.